The Diphosphate Monoanion in the Gas Phase: A Joint Mass Spectrometric and Theoretical Study

Andreina Ricci,*[a] Federico Pepi,[a] Marco Di Stefano,[b] and Marzio Rosi[b]

Abstract: $H_3P_2O_7^-$ ions were obtained in an electrospray ion source of a Fourier transform ion cyclotron resonance (ESI/FTICR) mass spectrometer from a CH_3CN/H_2O (1:1) pyrophosphoric acid solution and in the ionic source of a triple quadrupole (TQ) mass spectrometer from the chemical ionisation (CI) of pyrophosphoric acid introduced by a thermostatically controlled direct insertion probe. The ions were structurally characterised by mass spectrometric techniques and theoretical calculations. Consistent with collisionally activated dissociation (CAD) mass spectrometric results, theoretical calculations identified the linear diphosphate anion (**I**) as the most stable isomer on the $H_3P_2O_7^-$ potential energy surface. The joint application of mass spectrometric techniques and theoretical methods provided information on the dissociative processes of diphosphate anions in the gas phase. Finally, this study provides an insight into the structures and stabilities of the $[H_3PO_4\cdots PO_3]^-$, $[HP_2O_6\cdots H_2O]^-$ and $[H_2PO_4\cdots HPO_3]^-$ clusters and allows the stability and structure of the dimetaphosphate anion, $HP_2O_6^-$, to be investigated at the B3LYP6-31+G* and CCSD(T) levels of theory.

Keywords: ab initio calculations · diphosphate anion · gas-phase chemistry · mass spectrometry · phosphate esters

Introduction

The hydrolysis of phosphate esters plays an essential role in biochemistry since the breaking of the P–O–P linkage represents the main energy resource of biosynthetic processes occurring within living cells.[1] Phosphate esters are an integral part of compounds that are fundamental to the maintenance of the life, ranging from genetic material and coenzymes to energy-storing compounds and signalling agents.

The inorganic diphosphate or pyrophosphate anion, $H_3P_2O_7^-$, is the simplest compound containing the P-O–P bond and, in spite of the differences between the chemistry of pyrophosphate and that of these "high-energy" molecules, it might represent a prototype for the understanding of factors controlling the hydrolysis of phosphate linkage esters in living organisms.

[a] Prof. A. Ricci, Dr. F. Pepi
Dip.to di Studi di Chimica e Tecnologia delle Sostanze Biologicamente Attive
Università di Roma "La Sapienza"
P.le A. Moro 5, 00185 Rome (Italy)
Fax: (+39) 649913602
E-mail: Andreina.Ricci@uniroma1.it

[b] Dr. M. D. Stefano, Prof. M. Rosi
Istituto per le Tecnologie Chimiche e Centro di Studi CNR "Calcolo Intensivo in Scienze Molecolari
c/o Dipartimento di Chimica, Università di Perugia
Via Elce di Sotto 8, 06123 Perugia (Italy)

However, despite the importance of these processes and the enormous number of studies carried out on this subject, numerous questions regarding the hydrolysis mechanism of phosphate esters are still open and a detailed understanding of the factors contributing to the resulting release of energy has still not been achieved.

It has long been known that condensed phosphates react with water to form simpler polyphosphates and, ultimately, orthophosphates.[2] The hydrolysis rate increases at higher temperatures, higher hydrogen ion concentrations and in the presence of cations and enzymes. However, one of the longer-standing questions is whether phosphate ester hydrolysis proceeds through an associative or a dissociative mechanism. In principle, two limiting mechanistic pathways can be envisaged to lead to the cleavage of the phosphoester bond of methylphosphate.[3–7]

The *dissociative* mechanism [Eq. (1)] proceeds via the hydrated metaphosphate ion PO_3^-, and the *associative* mechanism [Eq. (2)] requires the formation of an intermediate or transition state with a pentacovalent phosphorus.

$$ROPO_3H^- \longrightarrow ROH + PO_3^- \xrightarrow{+H_2O} ROH + H_2PO_4^- \quad (1)$$

$$ROPO_3H^- \xrightarrow{+H_2O} \begin{matrix} & OR & \\ & | & \\ HO-P & \cdots & O^- \\ & | & \\ & OH & \\ & OH & \end{matrix} \longrightarrow ROH + H_2PO_4^- \quad (2)$$

DOI: 10.1002/chem.200305329

The only experimental information on the anionic polyphosphate species in the gas phase refers to the hydration free energies of singly and doubly charged anions,[8] the electron-detachment energies of $H_2PO_4^-$, $H_2P_2O_7^{-2}$ and $H_3P_3O_{10}^{-2}$[9] as well as their quantitative analysis by electrospray mass spectrometry (ESI/MS).[10] The reactivity of trimethyl phosphate and of the conjugate base of dimethyl methyl phosphonate, $(CH_3O)_2POCH_2^-$, has been examined in the gas phase by the flowing afterglow technique.[11]

Furthermore, all the theoretical studies on $H_4P_2O_7$ and its anions have focused on their structures and on the structures of their complexes with singly and doubly charged metal ions.[12–17] The aim of these studies is to provide insights into the thermochemistry of the hydrolysis reaction, into the involvement of a metaphosphate intermediate, into the catalytic role of a Mg^{2+} cation and into solvation effects. However, all in-depth theoretical investigations of the mechanism of hydrolysis only addressed the methyl phosphate anion[3–5,18] and not the polyphosphate anions.

The present paper describes the preparation and structural characterisation of $H_3P_2O_7^-$ ions by the joint application of mass spectrometric techniques, electrospray ionisation Fourier transform ion cyclotron resonance and triple quadrupole mass spectrometry (ESI-FTICR/MS and TQ-MS) as well as theoretical methods. Furthermore, the study of gas-phase ion chemistry of $H_3P_2O_7^-$ ions is aimed at clarifying the factors affecting the stability and reactivity of polyphosphate species and at providing benchmarks for an enhanced comprehension of their liquid-phase chemical behaviour.

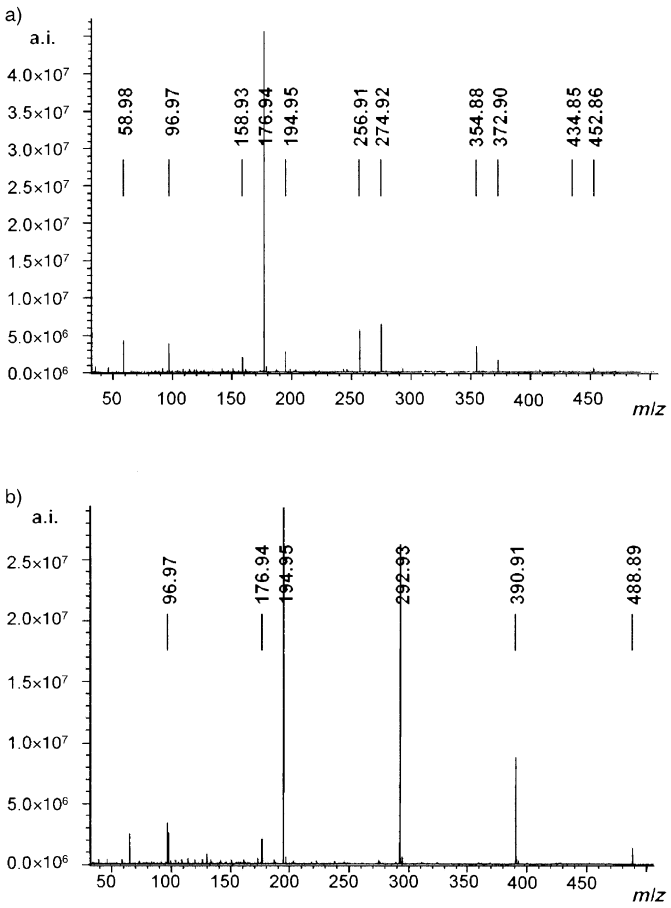

Figure 1. a) ESI spectrum of CH_3CN/H_2O (1:1) solution of $H_4P_2O_7$; b) ESI spectrum of CH_3CN/H_2O (1:1) solution of H_3PO_4

Results

Generation of the $H_3P_2O_7^-$ ions: The $H_3P_2O_7^-$ ion at *m*/*z* 177 is the most abundant species in the ESI spectrum of a CH_3CN/H_2O (1:1) pyrophosphoric acid solution (Figure 1a). A similar spectrum was obtained from CH_3OH/H_2O (1:1) or CH_3CN/H_2O(3% CH_3COOH) (1:1) solutions.

Besides the ion at *m*/*z* 177, the ESI spectrum of $H_4P_2O_7$ shows two kinds of ions which differ in their water content: the ions corresponding to the formal addition of one, two and three phosphoric acid molecules (*m*/*z* 275, 373, 471, respectively) and the ions arising by the loss of one water molecule from each of these species (*m*/*z* 257, 355, 453, respectively). When $H_2{}^{18}O$ was added to the ESI solutions, *no labelled water was incorporated*, thus confirming the purely dehydration nature of the formation process of the latter species.

Interestingly, $H_3P_2O_7^-$ ions at *m*/*z* 177 were also obtained at lower intensities from the ESI of phosphoric acid CH_3CN/H_2O solution (Figure 1b).

The spectrum shows the ions at *m*/*z* 195, 293, 391 and 489 corresponding to the addition of 1, 2, 3, and 4 phosphoric acid units, respectively, to the $H_2PO_4^-$ ion (*m*/*z* 97). The lack of corresponding dehydrated ionic species suggests a possible structural difference between these H_3PO_4 addition products and the species observed in the $H_4P_2O_7$ ESI spectrum resulting in a different ability to loose water. In all the solutions, the increase in the pyrophosphoric or phosphoric acid concentration leads to higher intensities of these ionic species.

In the triple quadrupole mass spectrometric experiments, $H_4P_2O_7$ or H_3PO_4 were introduced into the ionic source by a direct insertion probe thermostated at 200 °C. The $H_3P_2O_7^-$ ions were generated by chemical ionisation with CH_4 or N_2O/CH_4 (1:1) as the bath gas. The CI spectra of $H_4P_2O_7$ and H_3PO_4 (Figure 2) display the same peaks but differ in their ionic intensities.

It is worth noting that the spectrum of H_3PO_4 exhibits the $H_3P_2O_7^-$ ion at *m*/*z* 177, besides the ion at *m*/*z* 97, $H_2PO_4^-$, which is present at high intensities. Among all other ions, the peaks at *m*/*z* 239 and at *m*/*z* 319 could correspond to condensed inorganic phosphates, such as trimetaphosphate, $H_2P_3O_9^-$, and tetrametaphosphate, $H_3P_4O_{12}^-$ ions, respectively.[2c]

Structural characterisation of the $H_3P_2O_7^-$ ions: Collisionally activated dissociation (CAD) mass spectrometry carried out with both the FT-ICR and TQ mass spectrometers was used to obtain information on the structure of $H_3P_2O_7^-$ ions.

Taking into account the experimental and theoretical results (vide infra), we examined four groups **I**–**IV** of structural isomers that have the $H_3P_2O_7^-$ formula.

Group (**I**) comprises the linear $H_3P_2O_7^-$ ions arising from direct deprotonation of diphosphoric acid. All the other

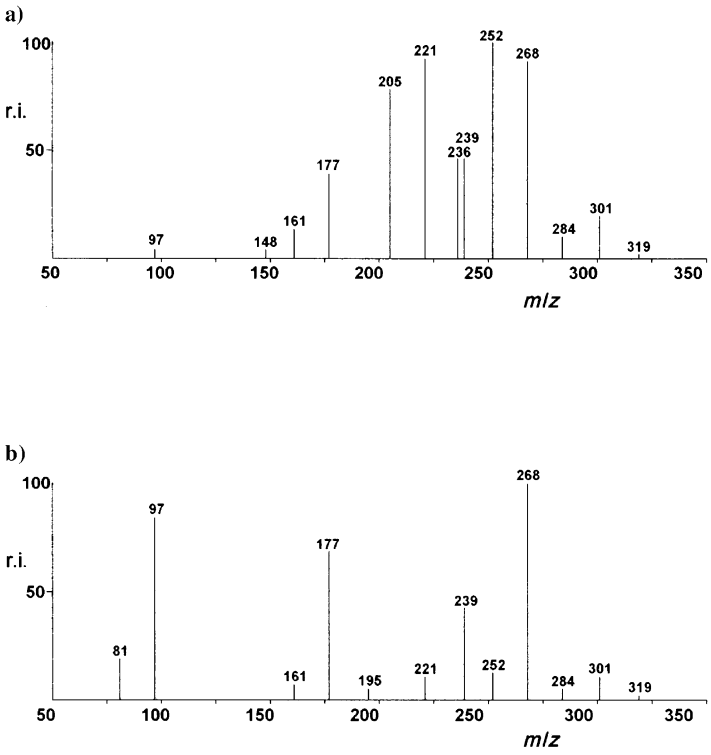

Figure 2. a) CI/CH_4 spectrum of $H_4P_2O_7$; b) CI/CH_4 spectrum of H_3PO_4

$[H_3P_2O_7]^-$ $[H_3PO_4\cdots PO_3]^-$ $[HP_2O_6\cdots H_2O]^-$ $[H_2PO_4\cdots HPO_3]^-$

I **II** **III** **IV**

groups include species characterised by cluster structures in which electrostatic interactions hold together the PO_3^- ion and phosphoric acid (**II**), the $HP_2O_6^-$ ion and a water molecule (**III**) and the $H_2PO_4^-$ ion and metaphosphoric acid (**IV**)

In the FT-ICR CAD experiments, the $H_3P_2O_7^-$ ions generated by the ESI process were transferred to the cell, isolated by soft ejection techniques and allowed to collide with argon after translational excitation with a suitable radio-frequency pulse. At low radio-frequency pulse intensity, the CAD spectrum of $H_3P_2O_7^-$ ions displayed only the PO_3^- fragment ion at *m*/*z* 79, corresponding to the loss of an H_3PO_4 molecule. If radio-frequency pulses of higher intensity were used, the abundance of the ion at *m*/*z* 79 increased and small amounts of the ion at *m*/*z* 159 were observed.

The same CAD spectrum was achieved for the ion at *m*/*z* 177 formed in the electrospray ionisation of phosphoric acid solution.

The energy-resolved TQ/CAD spectrum of the $H_3P_2O_7^-$ ions recorded at nominal collision energies ranging from 0–50 eV (laboratory frame) is reported in Figure 3.

Under low collision-energy conditions, the spectrum displayed the fragment at *m*/*z* 159, $HP_2O_6^-$, corresponding to the loss of a water molecule. At slightly higher collision energies, it displayed the ion at *m*/*z* 79, PO_3^-, corresponding to the loss of H_3PO_4. As the collision energies were increased, this ion became the most important fragmentation channel with a relative intensity of 62.4% at 30 eV. The ion at *m*/*z* 97, $H_2PO_4^-$, corresponding to the loss of HPO_3, appears only at collision energies above 20 eV. It is worth noting that the CAD spectra of the ions at *m*/*z* 177 obtained from pyrophosphoric and phosphoric acid are absolutely identical.

The reactivity of $H_3P_2O_7^-$ ions: The reactivity of $H_3P_2O_7^-$ ions toward different substrates is reported in Table 1, which shows also the substrate acidity value and the relative efficiencies of the observed reactions.

Under the low-pressure conditions of the FT-ICR experiments (10^{-7}–10^{-8} mbar), $H_3P_2O_7^-$ ions are inert toward compounds such as H_2O, alcohols (CH_3OH, C_2H_5OH, CF_3CH_2OH) and ketones (CH_3COCH_3). Traces of the $CF_3COCH_2^-$ ion are detected from the reaction between $H_3P_2O_7^-$ ions and CF_3COCH_3. Besides the proton transfer reaction, an addition product is formed from the reaction between $H_3P_2O_7^-$ ions and CF_3COOH. The reactivity of pyrophosphate monoanion was also tested toward $H_2{}^{18}O$, $Si(CH_3)_3N_3$ and $Si(CH_3)_3Cl$, to gather additional information on its structure. The chemical inertness of $H_3P_2O_7^-$ ion toward water in the gas phase at the low pressure conditions of FTICR experiments was confirmed by the absence of any

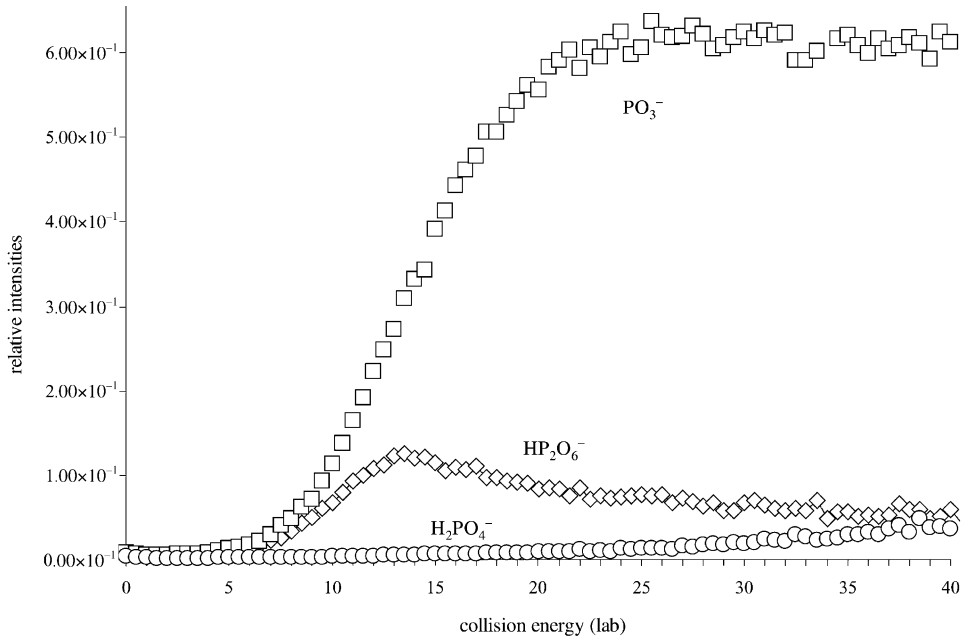

Figure 3. Energy-resolved TQ/CAD spectrum of the $H_3P_2O_7^-$ ions from $H_4P_2O_7/CH_4$/CI

Table 1. Observed pathways and relative efficiencies for reactions of selected compounds with $H_3P_2O_7^-$ ions.

Reference compound (AH)	Product anion	Reaction type	$\Delta H°_{acid}$ (AH) [kcal mol^{-1}]	Reaction efficiency [%]
H_2O	–	no reaction	390.7	–
CH_3OH	–	no reaction	382.0	–
C_2H_5OH	–	no reaction	378.3	–
CF_3CH_2OH	–	no reaction	361.7	–
CH_3COCH_3	–	no reaction	367.6	–
CF_3COCH_3	*traces of* $CF_3COCH_2^-$	PT[a]	350.3	–
CH_3COOH	–	no reaction	348.1	–
CF_3COOH	$[CF_3COOH, H_3P_2O_7]^-$	CL, PT[a]	323.8	≈10 %
$SiMe_3N_3$	$[SiMe_3H_2P_2O_7]^-$	addition/ HN_3 elimination	–	≈0.5 %
$SiMe_3Cl$	$[SiMe_3H_2P_2O_7]^-$	addition/ HCl elimination	–	≈0.5 %

[a] PT = proton transfer, CL = clustering. [b] Values from ref. [28].

Table 2. Thermochemical parameters [kcal mol^{-1}] for the isomerisation processes of the investigated anions. We report both the B3LYP and the CCSD(T) values calculated with the 6-31+G* basis set.

Reaction	B3LYP		CCSD(T)	
	ΔH	ΔH^+	ΔH	ΔH^+
Ia→**Ib**	0.3	28.7	0.3	31.2
Ia→**Ic**	12.7	26.9	13.7	35.8
Ia→**IIa**	13.7	32.6	18.1	36.9
Ia→**IIIa**	17.4	41.8	16.8	42.1
Ia→**IVa**	26.7	39.2	28.2	42.5
Ib→**IIId**	37.3	44.7	39.2	49.8
IIa→**IIb**	1.1	29.9	1.3	33.5
IIb→**IIc**	2.1	34.8	0.7	43.0
IIIa→**IIIb**	−0.8	–	−0.8	–
IIIb→**IIIc**	1.8	–	1.9	–
IIId→**IIIe**	−3.3	–	−3.7	–
IIIe→**IIIf**	2.8	–	2.7	–
IVa→**IVb**	10.0	–	13.7	–
IVb→**IVc**	0.00	–	0.00	–

Table 3. Thermochemical parameters [kcal mol^{-1}] for the barrierless fragmentation processes of interest. We report both the B3LYP and the CCSD(T) values calculated with the 6-31+G* basis set.

Reaction	B3LYP ΔH	CCSD(T) ΔH
IIa→PO_3^- + H_3PO_4	34.1	36.5
Ic→$HP_2O_6^-$ + H_2O	36.1	38.9
IIIa→$HP_2O_{6\,(a)}^-$ + H_2O	10.1	11.4
IIId→$HP_2O_{6\,(b)}^-$ + H_2O	11.2	13.1
IVa→$H_2PO_4^-$ + HPO_3	37.0	41.4

product incorporating heavy oxygen when $H_2{}^{18}O$ was introduced in the cell.

The reaction with $Si(CH_3)_3N_3$ and $Si(CH_3)_3Cl$ leads to the formation of an ion at *m*/*z* 249 arising from the addition of the trimethylsilyl group and the elimination of an HN_3 or HCl molecule, respectively.

Theoretical calculations: At the B3LYP/6-31+G* level of theory, the analysis of the $H_3P_2O_7^-$ potential energy surface led to the characterisation of numerous structural isomers of the species of interest. In particular, in accordance with the experimental hypothesis, we were able to optimise four different groups of structures (**I**–**IV**) showing either a linear or a cluster geometry and each one of them will be described separately. Inside every group, each isomer was been named with the group number followed by a letter: the lowest energy species was labelled as **a**, while all the other isomers investigated were labelled as **b**, **c**, etc.

Table 2 gives the thermochemical parameters for the isomerisation processes among the investigated species. Table 3 gives the dissociation energies of all investigated clusters.

The $H_3P_2O_7^-$ ions, group I: In Figure 4, we report the optimised geometries at the B3LYP/6-31+G* level of theory of the linear $H_3P_2O_7^-$ ions arising from direct deprotonation of pyrophosphoric acid.

The structure of the species lowest in energy, **Ia**, is in good agreement with previous investigations,[12–15] although some slight differences can be observed in bond lengths and angles owing to the choice of the basis set and theoretical methods. It is worth noting that this isomer presents two electrostatic interactions between the OH hydrogens and two oxygen atoms. By shifting one hydrogen, **Ia** can evolve into **Ib** or **Ic**. While the first transformation is practically thermoneutral, the isomerisation of **Ia** to **Ic** is endothermic by 13.7 kcal mol^{-1} (Table 2). The activation enthalpy for

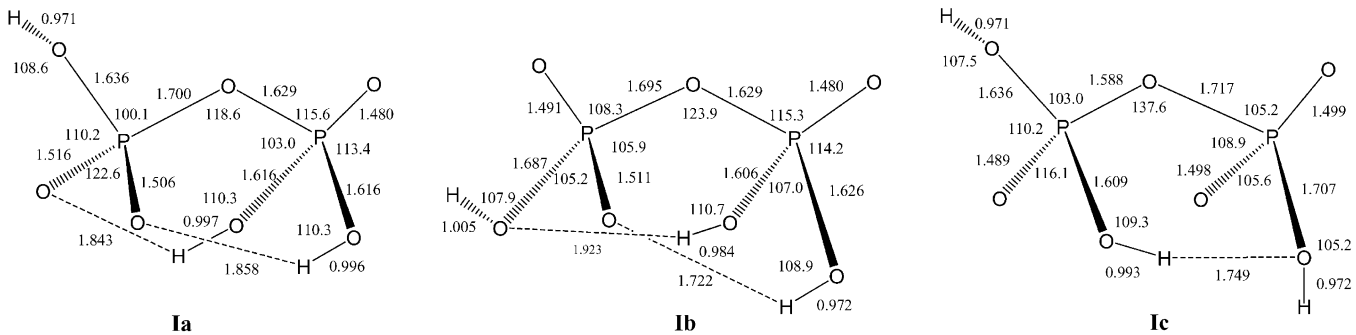

Figure 4. Optimised geometry (bond lengths [Å] and angles [°]) of the $H_3P_2O_7^-$ ions at the B3LYP/6-31+G* level of theory.

these two processes are, however, comparable: the calculated values are 31.2 and 35.8 kcal mol^{-1}, respectively.

The $[H_3PO_4\cdots PO_3]^-$ clusters, group II: In Figure 5, we report the optimised geometries at B3LYP/6-31+G* level of theory for the investigated clusters showing both fragments connected to each other by electrostatic interactions. Moreover, they are all isoenergetic (Table 2). The species lowest in energy, labelled **IIa**, differs from cluster **IIb** for a different coordination of the hydrogen atom. In the third structure, **IIc**, we note three electrostatic interactions *involving the same oxygen atom* of PO_3^-.

The $[HP_2O_6\cdots H_2O]^-$ clusters, group III: Figure 6 shows two isomeric forms of the anion $HP_2O_6^-$. In the structure labelled $HP_2O_6^-{}_{(b)}$ we can still observe the pyrophosphate linkage P–O–P, whose bond angle is 131.4°.

Of particular interest is the second structure labelled as $HP_2O_6^-{}_{(a)}$. An analysis of its geometry shows that it has a four-membered ring structure in which both P atoms are connected to each other by two O–P bonds. The P-O-P angle is bent to 92.5°and a weak H–O interaction is calculated (2.383 Å). From the energetic point of view, at CCSD(T)/6-31+G* level of theory, the energy of the latter species lies 24.4 kcal mol^{-1} below that of the first structure. However, in the search for a possible clustering with H_2O, we focussed on both fragments: the first one appeared to be a likely candidate because it allowed the general pyrophosphate structure to be preserved; conversely, the second anion would allow us to investigate less energetic clusters and fragmentation pathways. Actually, considering the potential energy surface of interest, we were able to optimise and characterise numerous clusters that have both fragments coordinated to H_2O.

Before considering them separately, it is worth mentioning that, whatever the coordination, we never observed any strong energetic variation. This means that the total energy of the cluster does not change with the coordination of H_2O. Moreover, the clusters containing $HP_2O_6^-{}_{(a)}$ as a central skeleton, that is **IIIa**, **IIIb** and **IIIc**, are more stable by nearly 25.0 kcal mol^{-1} than the clusters **IIId**, **IIIe** and **IIIf**, which contain the $HP_2O_6^-{}_{(b)}$ moiety. Thus, the same behaviour as the separate anions is observed. Figure 7 shows the optimised geometries at the B3LYP/6-31+G* level of theory for all clusters investigated. It is quite apparent that the coordination of the water molecule does not lead to substantial changes in the fragment's geometry and, in all cases, the interactions are rather weak and involve the H_2O hydrogens and the oxygens of the central anion. Such an electrostatic interaction can easily be broken in barrierless processes.

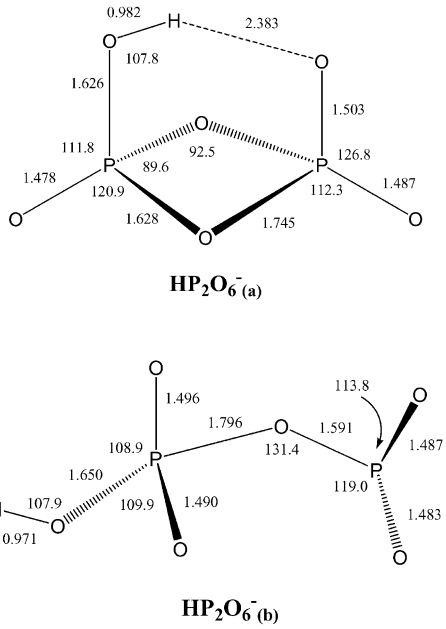

Figure 6. Optimised geometries (bond lengths [Å] and angles [°]) of the $HP_2O_6^-$ isomers at the B3LYP/6-31+G* level of theory.

The $[H_2PO_4\cdots HPO_3]^-$ cluster, group IV: We investigated three clusters, whose geometries at the B3LYP/6-31+G* level of theory are drawn in Figure 8. In all of them, we observed electrostatic interactions linking both fragments, although their spatial orientation is different. Structure **IVa**, the most stable of the group, is characterised by three electrostatic interactions. Isomers **IVb** and **IVc** show only one electrostatic interaction which involves the HPO_3 hydrogen and one OH group of $H_2PO_4^-$.

The energetic and structural information provided by the theoretically investigated species are summarised in the potential energy profile illustrated in Figure 9, the transition structures for clusters formation from linear anions are reported in Figure 10.

First, we consider the dissociation of $H_3P_2O_7^-$ ions, **Ia**, into the PO_3^- ions. This pathway is important because, in principle, the reactions of the singly charged diphosphate anion resulting in hydrolysis or transfer of the phosphoryl

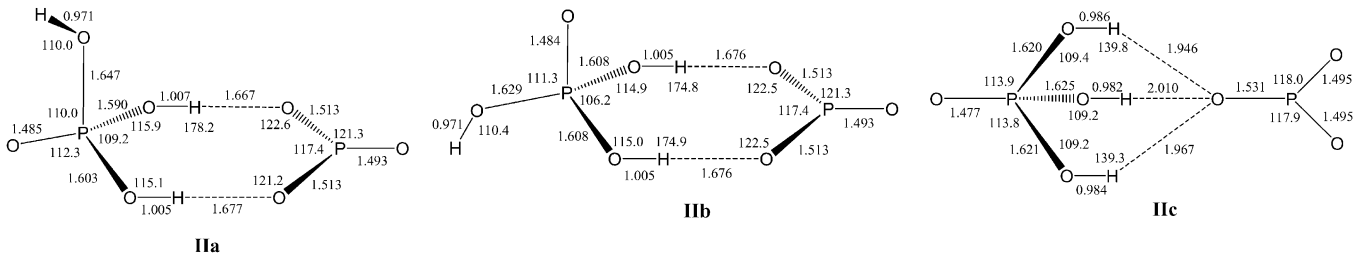

Figure 5. Optimised geometries (bond lengths [Å] and angles [°]) of the $[H_3PO_4\cdots PO_3]^-$ clusters, group **II** at the B3LYP/6-31+G* level of theory.

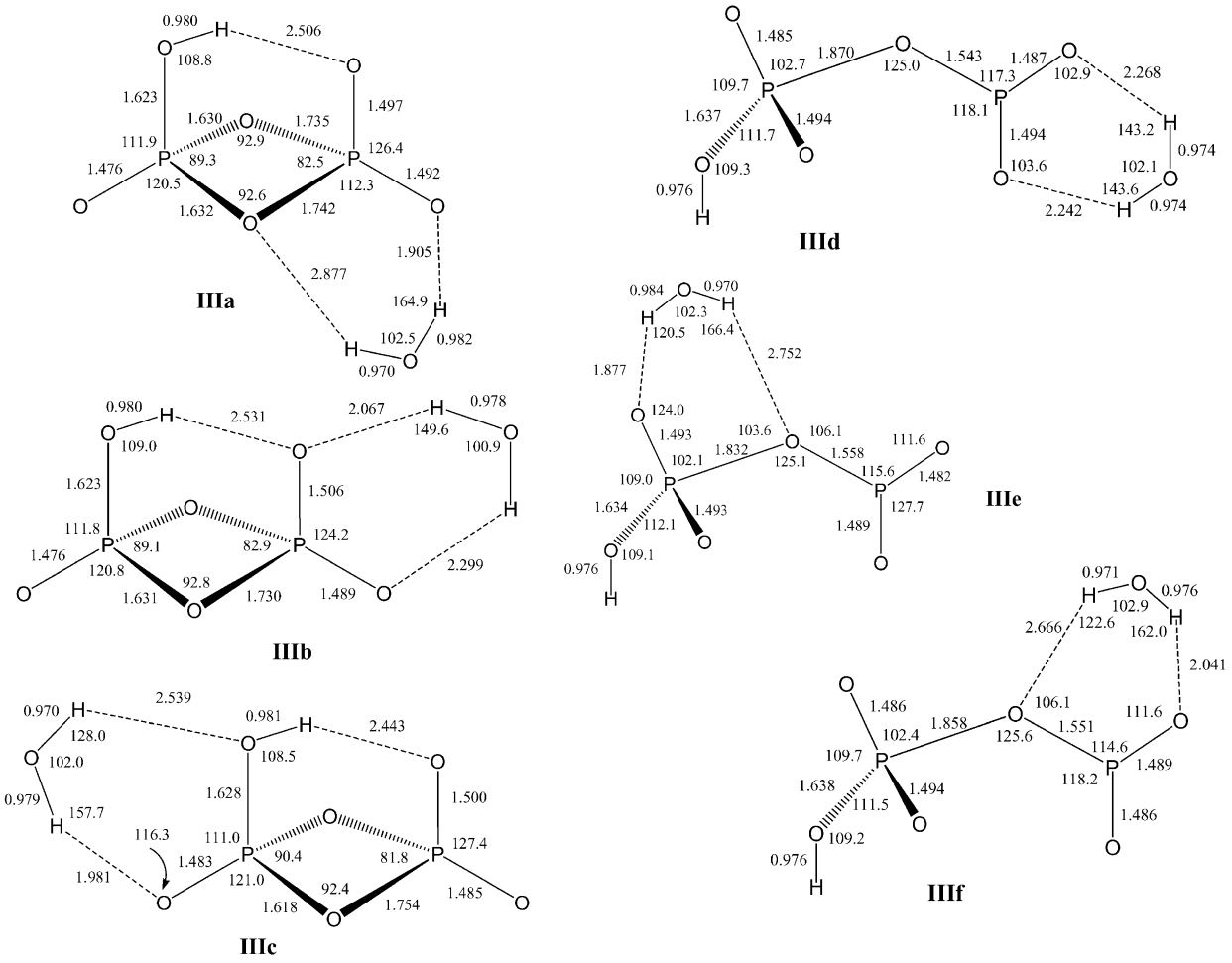

Figure 7. Optimised geometries (bond lengths [Å] and angles [°])of the $[HP_2O_6 \cdots H_2O]^-$ clusters, group **III**, at the B3LYP6-31+G* level of theory.

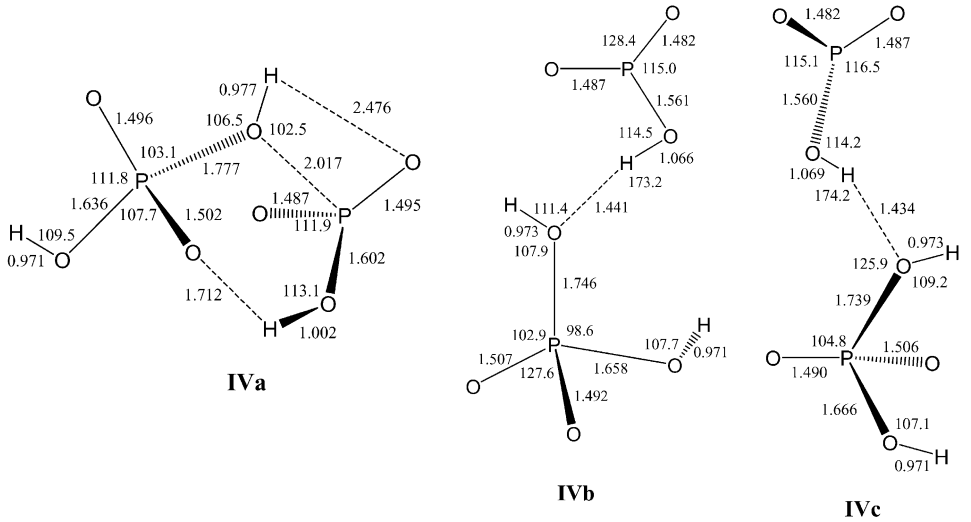

Figure 8. Optimised geometries (bond lengths [Å] and angles [°]) of the $[H_2PO_4 \cdots HPO_3]^-$ clusters, group **IV** at B3LYP/6-31+G* level of theory.

group can occur, analogously to phosphate monoesters, by a dissociative mechanism [Eq. (1)]. The simplest possible reaction mechanism leading to the dissociation of the diphosphate anion to PO_3^- and phosphoric acid involves an intramolecular proton-transfer process proceeding via the four-membered transition state **TS1** (Figure 10). The isomerisation of $H_3P_2O_7^-$ ions, **Ia**, into the $[H_3PO_4 \cdots PO_3]^-$ cluster, **IIa**, was computed to be endothermic by 18.1 kcal mol^{-1} with a barrier height of 36.9 kcal mol^{-1} at the CCSD(T)/6-31+G* level of theory. From the dissociation energy of **IIa**, reported in Table 3 and amounting to 36.5 kcal mol^{-1}, the overall dissociation process is found to be endothermic by 54.6 kcal mol^{-1}.

As in the previous case, the isomerisation of **Ia** ions to $[H_2PO_4 \cdots HPO_3]^-$ cluster, **IVa**, proceeds via a proton transfer to the bridging oxygen but involves the shift of a different H atom. This process is endothermic by 28.2 kcal mol^{-1} and has an activation barrier, referred to as the **TS4** transition state (Figure 10), of 42.5 kcal mol^{-1}. Considering that the release of $H_2PO_4^-$ from

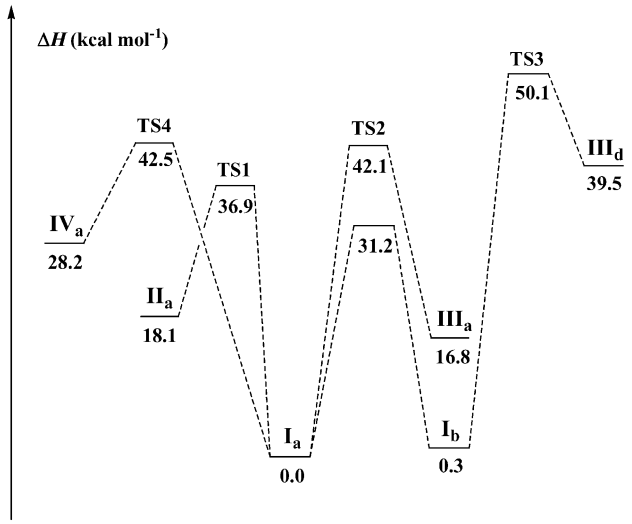

Figure 9. Schematic representation at the CCSD(T)/6-31+G* level of theory of the relative stabilities of the investigated species. All thermochemical parameters are in kcal mol^{-1}.

IVa requires 41.4 kcal mol^{-1}, the overall dissociation is found to be endothermic by 69.6 kcal mol^{-1}.

The cyclisation of the diphosphate anion as a result of the internal nucleophilic attack of an oxygen on the opposite phosphorus atom and by a proton shift between the OH groups bound to this phosphorus, leads to the isomerisation of **Ia** into the cluster $[HP_2O_{6(a)}\cdots H_2O]^-$, **IIIa**, through the transition state **TS2** (Figure 10). This process is endothermic by 16.8 kcal mol^{-1} and has an activation barrier of 42.1 kcal mol^{-1}. From the dissociation energy of the cluster, 11.4 kcal mol^{-1}, the overall process requires 28.2 kcal mol^{-1}.

It should be noted that a cluster between the linear $HP_2O_6^{-}{}_{(b)}$ and H_2O, **IIId**, could also be formed from the $H_3P_2O_7^-$ ion, **Ib**. This isomerisation is computed to be endothermic by 39.2 kcal mol^{-1} and characterised by an activation barrier of 49.8 kcal mol^{-1}. As can be seen from Table 3, the dissociation energy of cluster **IIId** amounts to 13.1 kcal mol^{-1} and the overall endothermicity is found to be 52.3 kcal mol^{-1}.

Finally, **Ic** can dissociate into the $HP_2O_6^{-}{}_{(b)}$ ion and H_2O, by a process, computed to be endothermic by 38.9 kcal mol^{-1}.

Discussion

The mechanistic and energetic picture of gas-phase ion chemistry of $H_3P_2O_7^-$ ions emerging from theoretical calculations is consistent with the experimental results and allows them to be rationalised.

Electrospray ionisation is a choice method for accomplishing the mass determination of biomolecules[20] in that the soft nature of this process allows the analyte to be observed as intact molecular ions with minimum fragmentation. On the basis of these considerations, it can reasonably be assumed that the $H_3P_2O_7^-$ ions generated from electrospray ionisation of pyrophosphoric acid solution and investigated by FTICR mass spectrometry maintain the structure of their precursor and hence are characterised by the structure labelled as **I**. However, although isomerisation processes leading

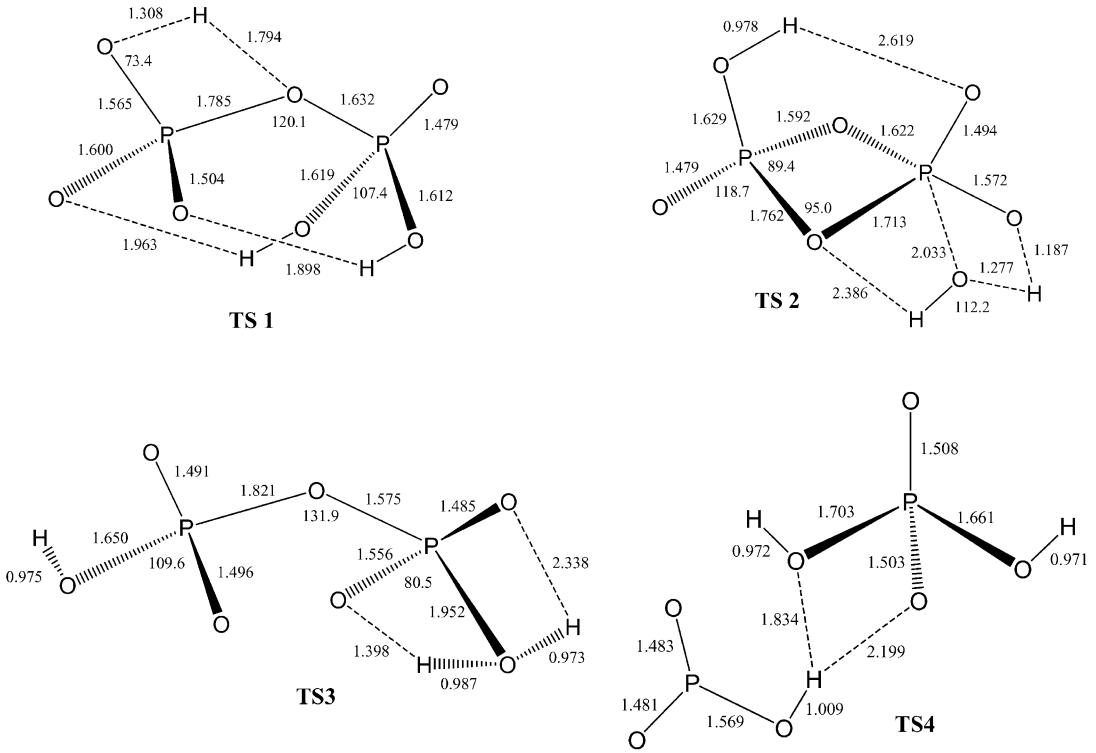

Figure 10. Optimised geometries (bond lengths [Å] and angles [°]) of the transition states (**TS 1–4**) at B3LYP6-31+G* level of theory.

to ion–molecule adducts are an unlikely event, the ability of the electrospray ionisation process to generate solvated ions necessitates a thorough structural characterisation of the ionic species of interest.

In the absence of model ions of known connectivity, we were able to characterise the $H_3P_2O_7^-$ structure on the basis of energetic considerations utilising energy-resolved CAD spectra. By considering the dissociation energies reported we actually observed that the most favoured decomposition channel of the $H_3P_2O_7^-$ clusters is represented by slight endothermic fragmentation into the $HP_2O_6^-$ ions at *m*/*z* 159 (11.4 kcal mol^{-1}), followed by fragmentation into the PO_3^- ions at *m*/*z* 79 (36.5 kcal mol^{-1}) and finally by the formation of the $H_2PO_4^-$ ion at *m*/*z* 97 (41.4 kcal mol^{-1}). The dissociation sequence of the $H_3P_2O_7^-$ ions, **I**, exactly follows the same order requiring 42.1, 54.6 and 69.6 kcal mol^{-1} for the fragmentation into $HP_2O_6^-$, PO_3^- and $H_2PO_4^-$ ions, respectively. Fortunately, even if the dissociation order for cluster and linear ions is the same, the dissociation energies of the $[HP_2O_6\cdots H_2O]^-$ clusters, **III**, are far lower than those of the $[H_3PO_4\cdots PO_3]^-$ isomers of group **II**. In the FT-ICR CAD mass spectra, the appearance of the $HP_2O_6^-$ ion (*m*/*z* 159) at energies higher than that of the PO_3^- fragment suggests the presence of the $H_3P_2O_7^-$ ions, **I**. This allows the existence of the $[HP_2O_6\cdots H_2O]^-$ cluster to be ruled out.

However, the formation of the PO_3^- fragment at low radio-frequency pulse intensity and its appearance during the first few seconds of reaction time, together with the drastic decrease in ionic signal during the isolation procedure could reasonably account for the endothermic dissociation of the $[H_3PO_4\cdots PO_3]^-$ cluster, (**II**).

With regard to the TQ/MS CAD experiments, it should be noted that the $H_3P_2O_7^-$ ions generated from CI of pyrophosphoric or phosphoric acid in the source of the triple quadrupole mass spectrometer are characterised by the same structure since their CAD mass spectra are identical.

To answer the question regarding the existence and the nature of the ions at *m*/*z* 177 in the chemical ionisation plasma containing H_3PO_4 we need to consider reaction (3), which, in the opposite direction, represents the long-debated hydrolysis of the diphosphate ion.

$$H_3PO_4 + H_2PO_4^- \rightarrow H_3P_2O_7^- + H_2O \qquad (3)$$

The $H_2PO_4^-$ ions formed through dissociative electron detachment process in the CI/CH_4 of H_3PO_4 can lead to the formation of the $H_3P_2O_7^-$ by the highly exothermic reaction [Eq. (3)] considering that the enthalpy change of the hydrolysis reaction (vide infra) was computed to be endothermic by nearly 23 kcal mol^{-1}.[12–15] Under low collision-energy conditions, the CAD spectra of $H_3P_2O_7^-$ ions display $HP_2O_6^-$ ions at *m*/*z* 159, which corresponds to the loss of a water molecule, and at slightly higher collision energies, the PO_3^- ion at *m*/*z* 79, which corresponds to the loss of H_3PO_4. Only at higher collision energies (>20 eV) does the $H_2PO_4^-$ ion appear (*m*/*z* 97), which corresponds to the loss of the HPO_3 molecule.

These results suggest that $H_3P_2O_7^-$ ions investigated by TQ/MS have the structure of the linear pyrophosphate anion **I**, the only structure which is consistent with the high-energy loss of the $H_2PO_4^-$ fragment. Furthermore, the appearance of both the ions at *m*/*z* 159 and *m*/*z* 79 at comparable energy thresholds allows the presence of the $[HP_2O_6\cdots H_2O]^-$ cluster **III** to be excluded.

Moreover, accurate measurements and carefully calibrated empirical fitting procedures[21] were required to obtain predictive values to the bonding energies from threshold curves. In the present research we obtained structural and energetic information from a qualitative analysis of the energy-resolved CAD spectra and hence we cannot discriminate between the ions **I** and the cluster **III** which decompose at similar energies.

These considerations allow us to assign to the ions at *m*/*z* 177, resulting from the CI plasma of TQ/MS and from the ESI process in the FT-ICR experiments, the linear structure **I** of the pyrophosphate anion, and points to the existence of the cluster species **II**, certainly in the latter conditions.

The low reactivity observed in the FT-ICR experiments characterises the pyrophosphate anion in the gas phase as a very stable inorganic species in accordance with its computed structure, which is found to be strongly stabilised by two internal hydrogen bonds.

Examination of the reaction efficiencies reported in Table 1 reveals that all the reactions of $H_3P_2O_7^-$ ions are generally inefficient. Clustering and proton transfer products have been observed with substrates characterised by a gas-phase acidity value close to that of $H_4P_2O_7$ and amounting to 323 kcal mol^{-1}.[12,15]

The $H_3P_2O_7^-$ ions react with $(CH_3)_3SiCl$ and $(CH_3)_3SiN_3$ yielding $[H_2P_2O_7\text{-}(CH_3)_3Si]^-$ ions, in agreement with previous observations[22] showing that nucleophiles with a proton affinity lower than that of Cl^- ($\Delta H°_{acid}$ HCl = 333.4 kcal mol^{-1}) react with $(CH_3)SiCl$ by an addition/HCl elimination process that is more strongly energetically favoured than an S_N2 mechanism. This reaction, which is analogous to the reaction of hydroxide ion with tetramethylsilane,[23] was also observed for singly charged phosphorylated oligonucleotides.[22] A pentacoordinate adduct, arising from the nucleophilic attack of an oxygen on the Si atom, is probably involved. It decomposes by elimination of a Cl^- anion and subsequent deprotonation of the incipient trimethylsilyldiphosphoric acid. The absence of products arising from the reaction between the $H_3P_2O_7^-$ anions and H_2O confirms the previous theoretical estimates on the endothermicity of the hydrolysis reaction and strengthens George's hypothesis[24] as to why compounds such as pyrophosphate and ATP are rich in energy. On the basis of calorimetric measurements in aqueous solution, George[24] was the first to suggest that the free energy of the hydrolysis of various pyrophosphate species almost entirely results from different heats of solution of reagents and products involved in the reaction and not to the relative energies of isolated molecules in vacuo. Indeed, whereas in the gas phase the hydrolysis of diphosphate monoanion was computed to be endothermic,[12–15] in solution the reaction was measured to be exothermic by −7.5 kcal mol^{-1}.[24]

It is known that condensed phosphates fall into the following three groups[2c]: 1) metaphosphates $M^I_n(PO_3)_n$ with

cyclic anions, 2) polyphosphate $M^{I}_{n+2}(P_nO_{3n+1})$ or $M^{I}_{n}H_2(P_nO_{3n+1})$ with open-chain anions in which each of the n tetrahedral PO_4 units (except those at the chain ends) is linked to each of its neighbours by an oxygen atom and 3) cross-linked phosphates or ultra phosphates containing "tertiary" P atoms that are linked to three other P atoms by three O atoms.

Polyphosphates are stable in aqueous solution at pH≈7 and 25 °C, but they are degraded at higher temperatures, higher hydrogen ion concentrations and in the presence of cations. The degradation leads to the formation of oligomers from the removal of monophosphate units, one at a time, from the chain ends or else yields cyclic metaphosphates, particularly trimetaphosphate, by the rearrangement of the folded polyphosphate chains. This second degradation route becomes more important as the polyphosphate chain-length increases.

In the gas phase, the induced dissociation of the diphosphate anion seems to occur through both degradation pathways leading to the formation of PO_3^- and cyclic $HP_2O_6^-$, which suggests that there is already a tendency for dimeric phosphates to cyclise.

Whereas the first member of the metaphosphates group, the monomeric PO_3^- ion, has been the subject of many experimental and theoretical studies owing to its role in biological systems[25] little is known about the dimeric $P_2O_6^{-2}$ ion.

The dimetaphosphate or cyclo-diphosphate dianion, $P_2O_6^{-2}$, was cited as an intermediate in the hydrolysis of adenosine 5′-*o*-(*S*-methyl-1-thiotriphosphate)[26a] and, recently, as an ionic fragment of CAD spectra of phosphorylated species.[26b] In the present study, we first used theoretical methods to study the structure of the $HP_2O_6^-$ ion, the ionic product of the gas-phase-induced dehydration of diphosphate anion. We found that a four-membered ring structure, in which both P atoms are connected to each other by two P–O bonds, makes the cyclic $HP_2O_6^-{}_{(a)}$ ion 24.4 kcal mol^{-1} more stable than the linear $HP_2O_6^-{}_{(b)}$.

As far as the isomerisation of linear ion **Ia** into the $[PO_3\cdots H_3PO_4]^-$ cluster **IIa** is concerned, in agreement with the correlation between acidity and solvation energy,[27] which indicates that the bond strength in hydrogen-bonded complexes ($XH\cdots A^-$) increases with the gas-phase acidity of XH and the gas-phase basicity of A^-, the dissociation energy of the $[PO_3\cdots H_3PO_4]^-$ cluster ($\Delta H°_{acid}$ (H_3PO_4) = 344 kcal mol^{-1})[19] reported in this work is found to be almost three times higher than the dissociation energy of the $[PO_3\cdots H_2O]^-$ cluster ($\Delta H°_{acid}$ (H_2O) = 390 kcal mol^{-1}),[19] which was estimated to be 12.9 kcal mol^{-1}.[25] Theoretical calculations on the gas-phase dissociative hydrolysis of the methyl phosphate monoanion[3] computed the isomerisation of $CH_3OPO_3H^-$ to $[CH_3OH\cdots PO_3]^-$ to be endothermic by 10.7 kcal mol^{-1} and to have an activation enthalpy of 28.3 kcal mol^{-1}. The higher activation enthalpy and the endothermicity of the **Ia** isomerisation probably reflect the presence of hydrogen bonds in the $H_3P_2O_7^-$ ions as well as the different stability of solvated PO_3^- ions.

The tendency of polyphosphate ions to cyclise together with the higher stability of cyclic metaphosphate anions as the number of the ring atoms increases, is revealed in the CI spectra of phosphoric and diphosphoric acid by the presence of ions at *m*/*z* 239 and 319, probably corresponding to the monoanionic form of trimetaphosphate **A** and tetrametaphosphate **B** ions.

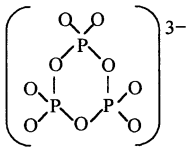

A

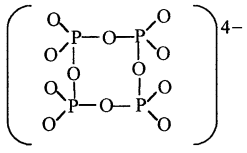

B

The orthophosphate and diphosphate anions, $H_2PO_4^-$ and $H_3P_2O_7^-$, belong to the second group of condensed phosphates, the linear polyphosphates.

The ability of phosphoric acid to form stable adducts and to undergo condensation reactions could explain the presence of anions of formula $[H_{3n-1}P_nO_{4n}]^-$, $[H_{n+1}P_nO_{3n+1}]^-$ and $[H_{3n-3}P_nO_{4n-1}]^-$ in the ESI spectra of phosphoric and pyrophosphoric acid.

Cross-linked phosphates, the third group of condensed phosphates, can be obtained by thermal dehydration of dihydrogen monophosphates and free phosphoric acid. The reactions involved are complex and depend on the nature of the cation as well as on the temperature and water vapour pressure.[2c] It is likely that these processes, occurring to a large extent under the CI conditions, were responsible for the formation of most of the ionic species observed in the CI spectra of phosphoric and diphosphoric acid.

Conclusion

The joint application of theoretical and experimental methods proved particularly fruitful in this study providing a detailed picture of the gas-phase ion chemistry of $H_3P_2O_7^-$ ions. Consistent with collisionally activated dissociation (CAD) mass spectrometric experiments, theoretical calculations identified the linear and covalently bound diphosphate anion (**I**) as the most stable isomer on the potential energy surface of $H_3P_2O_7^-$ ions.

Firstly, the structure of the $HP_2O_6^-$ ion, the dimetaphosphate or cyclo-diphosphate anion, was investigated by theoretical methods. For this ion, formed from the induced dehydration of diphosphate anion in the gas phase, we found that the cyclic isomer, $HP_2O_6^-{}_{(a)}$, characterised by a four-membered ring structure where both P atoms are connected to each other by two P–O bonds, is 24.4 kcal mol^{-1} more stable than the linear $HP_2O_6^-{}_{(b)}$ at the B3LYP/6-31+G* and CCSD(T) levels of theory.

This study reports the energetic profile of the gas-phase-induced dissociation of diphosphate ion. In this context, the dissociation into PO_3^- ions is important since it represents the first step of the dissociative mechanism [Eq. (1)] resulting in hydrolysis or transfer of a phosphoryl group.

The ability of the electrospray ionisation process to generate solvated ions allows this study to be extended to mono-

solvated and chelated species. Theoretical and experimental work is currently under way on $H_5P_2O_8^-$ and $M^IH_2P_2O_7^-$ ions and is aimed at evaluating the influence of a water molecule and of metal chelation on the reactivity of diphosphate anion.

Experimental Section

Materials: $H_4P_2O_7$ and all chemicals were obtained from Sigma-Aldrich Ltd.

Instrumentation. ESI-FTICR/MS experiments were performed with a Bruker BioApex 4.7T FT-ICR mass spectrometer equipped with an Analytica of Brandford Electrospray Ionisation Source. Samples were infused into a fused-silica capillary (i.d. 50 μm) at a flow rate of 130 $\mu L\,min^{-1}$, and the ions were accumulated in a hexapole ion guide for 0.8 s. Typical ESI voltages for cylinder, capillary and end plates were 3000, 4000, and 4300 V, respectively. The capillary exit and the skimmer which were set to −60 and −10 V, respectively, hexapole d.c. offset, 0.7 V.

Triple quadrupole mass spectra were recorded on a TSQ 700 mass spectrometer from Finnigan Ltd., operating in the negative-ion mode.

Methods: The $H_3P_2O_7^-$ ions were obtained in the electrospray ion source of a Fourier transform ion cyclotron resonance (FTICR) mass spectrometer from a CH_3CN/H_2O (1:1) pyrophosphoric acid solution. Polyphosphate solution samples were prepared daily at a concentration of 10^{-4} M. The $H_3P_2O_7^-$ ions were transferred into the resonance cell (25 °C) and isolated by broad band and "single shot" ejection pulses. After a thermalising delay time of 1–2 s, the ions were re-isolated by "single shots" and allowed to react with neutral reagents in the cell. The pressure of the neutral reactants, ranging from 10^{-8} to 10^{-7} mbar, was measured by a Bayard–Alpert ionisation gauge, whose readings were calibrated with the known rate coefficient of the $CH_4 + CH_4^+ \rightarrow CH_5^+ + CH_3$ reaction.[28] The readings were corrected for the relative sensitivity to the various gases used according to a standard method.[29] The pseudo-first-order rate constants were obtained by plotting the logarithm of $I_t/I_{t=0}$ ratio as a function of the reaction time. Then the bimolecular rate constants were determined from the number density of the neutral molecules, which were themselves inferred from the pressure of the gas. Average Dipole Orientation (ADO) collision rate constants (k_{ADO}) were calculated as described by Su and Bowers.[30] Reaction efficiencies are the ratio of k_{ADO}, the collision rate constants, to the experimental rate constants, k_{exp}. The uncertainty of each rate constant is estimated to be 30 %.

The $H_3P_2O_7^-$ ions were also obtained in the chemical ionisation (CI) source of a triple quadrupole mass spectrometer (TQ/MS) from pyrophosphoric acid introduced by a direct insertion probe thermostatically controlled at 200 °C. The CI of $H_4P_2O_7$ was accomplished by deprotonation by OH^- ions formed in a N_2O/CH_4 (1:1) gaseous mixture or by dissociative electron detachment in a CH_4 plasma. The ions of interest were driven into the collision cell, actually an RF-only hexapole, containing the neutral reagent. Collisionally activated dissociation (CAD) experiments were recorded utilizing Ar as the target gas at a pressure of $1–5 \times 10^{-5}$ Torr and at a collision energy ranging from 0 to 50 eV (laboratory frame). The charged products were analysed with the third quadrupole, scanned at a frequency of 150 amu s^{-1}.

Computational details: Density functional theory, based on the hybrid[31] B3LYP functional,[32] was used to localise the stationary points of the investigated systems and to evaluate the vibrational frequencies. Single-point energy calculations at the optimised geometries were performed with the coupled-cluster single and double excitation method[33] with a perturbational estimate of the triple excitations approach CCSD(T).[34] Zero-point energy corrections evaluated at the B3LYP level were added to the CCSD(T) energies. The zero total energies of the species of interest were corrected to 298.15 K by adding translational, rotational and vibrational contributions. The absolute entropies were calculated with standard statistical-mechanistic procedures from scaled harmonic frequencies and moments of inertia relative to B3LYP/6-31+G* optimised geometries. The 6-31+G* basis set[35] was used. All calculations were performed with the computational program Gaussian 98.[36]

Acknowledgments

The authors wish to express their gratitude to Professor Fulvio Cacace for his encouragement and helpful discussion. Financial support from the Italian Ministero dell' Universitàe della Ricerca Scientifica e Tecnologica (MURST) and from Consiglio Nazionale delle Ricerche (CNR) is gratefully acknowledged.

[1] F. H. Westheimer, *Science* **1987**, *235*, 1173.
[2] a) J. R. Van Wazer, E. J. Griffith, , J. F. McCullough, *J. Am. Chem. Soc.* **1955**, *77*, 287; b) M. Watanabe, *Bull. Chem. Soc. Jpn.* **1974**, *47*, 2048; c) E. Thilo, *Angew. Chem.* **1965**, *77*, 1056; *Angew. Chem. Int. Ed. Engl.* **1965**, *4*, 1061; d) J. B. Gill, S. A. Riaz, *J. Chem. Soc. A* **1969**, 844; e) R. Gupta, S. A. Rayeeny, S. S. Das, H. N. Bhargava, *Polym. Degrad. Stab.* **1995**, *50*,183; f) F. Rashchi, J. A. Finch, *Miner. Eng.* **2000**, *13*, 1019, and references therein.
[3] M. Bianciotto, J.-C. Barthelat, A. Vigroux, *J. Am. Chem. Soc.* **2002**, *124*, 7573, and references therein.
[4] J. Florian, A. Warshel, *J. Phys. Chem. B* **1998**, *102*, 719;
[5] C.-H. Hu, T. Brinck, *J. Phys. Chem. A* **1999**, *103*, 5379
[6] H.-K. de Jager, A. M. Heyns, *J. Phys. Chem. A* **1998**, *102*, 2838 and references therein.
[7] S. Admiraal, D. Herschlag, *J. Am. Chem. Soc.* **2000**, *122*, 2145
[8] A. T. Blades, H. Yeunghaw, P. Kebarle, *J. Phys. Chem.* **1996**, *100*, 2443
[9] X.-B. Wang, E. R. Vorpagel, X. Yang, L.-S. Wang, *J. Phys. Chem.* **2001**, *105*, 10468.
[10] B. K. Choi, D. M. Hercules, M. Houalla, *Anal. Chem.* **2000**, *72*, 5087.
[11] R. C. Lum, J. J. Grabowski, *J. Am. Chem. Soc.* **1992**, *114*, 8619, and references therein; b) R. C. Lum, J. J. Grabowski, *J. Am. Chem. Soc.* **1993**, *115*, 7823, and references therein
[12] D. M. Hayes, G. L. . Kenyon, P. A. Kollman, *J. Am. Chem. Soc.* **1978**, *100*, 4334; b) B. Ma, C. Meredith, H. F. Schaefer, III, *J. Phys. Chem.* **1994**, *98*, 8216.
[13] M. E. Colvin, E. Evleth, Y. Akacem, *J. Am. Chem. Soc.* **1995**, *117*, 4357.
[14] B. Ma, C. Meredith, H. F. Schaefer, III, *J. Phys. Chem.* **1995**, *99*, 3815.
[15] H. Saint-Martin, L. E. Ruiz-Vicent, A. Ramirez-Solìs, I. Ortega-Blake, *J. Am. Chem. Soc.* **1996**, *118*, 12167.
[16] H. Saint-Martin, L. E. Ruiz-Vicent, *J. Phys. Chem. A* **1999**, *103*, 6862
[17] W. J. McCarthy, D. M. A. Smith, L. Adamowicz, H. Saint-Martin, I. Ortega-Blake, *J. Am. Chem. Soc.* **1998**, *120*, 6113.
[18] M. Bianciotto, J. -C. Barthelat, A. Vigroux, *J. Phys. Chem. A* **2002**,*106*, 6521
[19] NIST Chemistry WebBook; NIST standard Reference Database No. 69, February **2000** release; data collection of the National Institute of Standards and Technology to be found under http://webbook.nist.gov
[20] N. B. Cech, C. G. Enke, *Mass Spectrom. Rev.* **2001**, *20*, 362–387, and references therein.
[21] a) P. B. Armentrout, *Int. J. Mass Spectrom.* **2000**, *200*, 219; b) P. B. Armentrout, *J. Am. Soc. Mass Spectrom.* **2002**, 13, 419, and references therein.
[22] R. A. J. O'Hair, S. C. McLuckey, *Int. J. Mass Spectrom. Ion Processes* **1997**, *162*, 183.
[23] J. C. Sheldon, R. N. Hayes, J. H. Bowie, C. H. DePuy, *J. Chem. Soc. Perkin Trans. 2* **1987**, 275.
[24] P. George, R. J. Witonsky, M. Trachtman, C. Wu, W. Dorwart, L. Richman, W. Richman, F. Shurayh, B. Lentz, *Biochim. Biophys. Acta* **1970**, *223*,1.
[25] a) R. G. Keese, A. W. Castleman, Jr., *J. Am. Chem. Soc.* **1989**, *111*, 9015; b) B. Ma, Y. Xie, M. Shen, H. F. Schaefer, III, *J. Am. Chem. Soc.* **1993**, *115*, 1943; c) B. Ma, Y. Xie, M. Shen, P. von R. Schleyer, H. F. Schaefer, III, *J. Am. Chem. Soc.* **1993**, *115*, 11169; d) A. T. Blades, Y. Ho, P. Kebarle, *J. Phys. Chem.* **1996**, *100*, 2443; e) R. A. Morris, A. A. Viggiano, *J. Chem. Phys.* **1998**, *109*, 4126.

[26] P. M. Cullis, M. B. Schilling, *J. Chem. Soc. Chem. Commun.* **1989**, *2*, 106; b) S. Gronert, R. A. J. O'Hair, *J. Am. Soc. Mass Spectrom.* **2002**, *13*, 1088
[27] A. T. Blades, J. S. Klassen, P. Kebarle, *J. Am. Chem. Soc.* **1995**, *117*, 10563; b) K. Takashima, J. M. Riveros, *Mass Spectrom. Rev.* **1998**, *17*, 409.
[28] Meot-Ner in *Gas Phase Ion Chemistry, Vol. 2* (Ed.: M. T. Bowers), Academic Press, New York, **1979**, pp. 198–268; b) Y. Ikezoe, S. Matsuoka, M. Takebe , A. A. Viggiano, *Gas Phase Reaction Rate Constants Through 1986*, Maruzen Co, Tokyo, Japan **1987**.
[29] J. E. Bartmess, R. M. Georgiadis, *Vacuum* **1983**, *33*, 149.
[30] T. Su, M. T. Bowers, *Int. J. Mass Spectrom. Ion Phys.* **1973**, *12*, 347
[31] A. D. Becke, *J. Chem. Phys.* **1993**, *98*, 5648.
[32] P. J. Stevens, F. J. Devlin, C. F. Chabalowski, M. J. Frisch, *J. Chem. Phys.* **1994**, *98*, 11623.
[33] R. Bartlett, *Annu. Rev. Phys. Chem.* **1981**, *32*, 359.
[34] K. Raghavachari, G. W. Trucks, J. A. Pople, M. Head-Gordon, *Chem. Phys. Lett.* **1989**, *157*, 479.
[35] R. Ditchfield, W. J. Hehre, J. A. Pople, *J. Chem. Phys.* **1971**, *54*, 724; b) W. J. Hehre, R. Ditchfield, J. A. Pople, *J. Chem. Phys.* **1972**, *56*, 2257; c) P. C. Hariharan, J. A. Pople, *Mol. Phys.* **1974**, *27*, 209; d) M. S. Gordon, *Chem. Phys. Lett.* **1980**, *76*, 163; e) P. C. Hariharan, J. A. Pople, *Theo. Chim. Acta* **1973**, *28*, 213; f) R. C. Binning, Jr., L. A. Curtiss, *J. Comput. Chem.* **1990**, *11*, 1206; g) T. Clark, J. Chandrasekhar, G. W. Spitznagel, P. von R. Schleyer, *J. Comput. Chem.* **1983**, *4*, 294; h) M. J. Frisch, J. A. Pople, J. S. Binkley, *J. Chem. Phys.* **1984**, *80*, 3265.
[36] M. J. Frisch, G. W. Trucks, H. B. Schlegel, G. E. Scuseria, M. A. Robb, J. R. Cheeseman, V. G. Zakrzewski, J. A. Montgomery, Jr, R. E. Stratmann, J. C. Burant, S. Dapprich, J. M. Millam, A. D. Daniels, K. N. Kudin, M. C. Strain, O. Farkas, J. Tomasi, V. Barone, M. Cossi, R. Cammi, B. Mennucci, C. Pomelli, C. Adamo, S. Clifford, J. Ochterski, G. A. Petersson, P. Y. Ayala, Q. Cui, K. Morokuma, D. K. Malick, A. D. Rabuck, K. Raghavachari, J. B. Foresman, J. Ciolowski, J. V. Ortiz, B. B. Stefanov, G. Liu, A. Liashenko, P. Piskorz, I. Komaromi, R. Gomperts, R. L. Martin, D. J. Fox, T. Keith, M. A. Al-Laham, C. Y. Peng, A. Nanayakkara, C. Gonzales, M. Challacombe, P. M. W. Gill, B. G. Johnson, W. Chen, M. W. Wong, J. L. Andres, M. Head-Gordon, E. S. Replogle, J. A. Pople, *Gaussian 98*, Revision A.7; Gaussian, Inc.: Pittsburgh, PA, **1998**.

Received: July 11, 2003
Revised: October 2, 2003 [F5329]